ORIGINAL ARTICLE

P. Novák · E. W. Grafarend

Ellipsoidal representation of the topographical potential and its vertical gradient

Abstract Due to the Global Positioning System (GPS), points on and above the Earth's surface are readily given by means of a triplet of the Gauss surface normal coordinates L, B and H called ellipsoidal longitude, ellipsoidal latitude, and ellipsoidal height, respectively. For geodetic applications, these curvilinear coordinates refer to the international reference ellipsoid GRS80, which is an equipotential surface of the Somigliana–Pizzetti reference potential field. Here, we aim at representing the gravitational potential, that is generated by the 'topographical' masses above GRS80, and its vertical gradient, i.e. an effect on measured gravity, in terms of the Gauss surface normal coordinates (L, B, H). The spatial (integral) formulas for the topographical potential and its vertical gradient are presented as a sum of a spherical term and corresponding ellipsoidal correction. The formulas for the terrain contribution are evaluated over the test area in the Canadian Rocky Mountains using an area-limited discrete integration. The spectral (series) representation of the topographical potential is also introduced, and the condensation of the topographical masses on or inside the reference ellipsoid is discussed in terms of a simple layer density. The ellipsoidal corrections might seem to be of limited significance in view of a relatively low accuracy of currently available topographical data, especially the mass density. However, the representation of the topographical potential and its vertical gradient using the coordinates that are directly observable with a high level of accuracy by GPS certainly has advantages.

Keywords Topography · Terrain · Gravitational potential · Reference ellipsoid · Ellipsoidal coordinates

P. Novák (✉) · E. W. Grafarend
Department of Geodesy and Geoinformatics,
Stuttgart University,
Geschwister-Scholl-Strasse 24/D, 70174 Stuttgart, Germany
E-mail: pnovak@pecny.asu.cas.cz
Fax: +420-323649236
Tel.: +420-323649235

P. Novák
Present address: Research Institute of Geodesy, Topography and Cartography, Department of Geodesy and Geodynamics, Prague-East, Czech Republic

1 Introduction

According to the spheroidal Bruns transform for local geoid determination (Grafarend et al. 1999), topographical masses are assumed to be bounded by the physical surface of the Earth and the reference ellipsoid. We first note that this definition is different from the conventional, where topography is defined as masses between the surface of the Earth and the geoid. Our topographical masses generate a gravitational potential called, herein, the topographical potential (TP). The evaluation of the TP and its vertical gradient (TPG) belongs to the traditional tasks of geodesy. Among other applications, the TP and TPG play an important role in the gravimetric determination of the geoid (reference equipotential surface of the Earth's gravity field) from gravity observations. The evaluation of the TP and TPG requires knowledge of geometry of the topographical masses in a selected coordinate system as well as their mass density distribution function.

This contribution deals with the theoretical formulation of the TP and TPG assuming that the topographical masses are described in the ellipsoidal coordinate system to which GPS-based (Global Positioning System) positions refer. Such derivations can be used for the numerical evaluation of the TP and TPG when the precise GPS-based positioning of the Earth's surface is available. Ellipsoidal coordinates also represent a natural choice when working with the reference ellipsoid. We anticipate that the ellipsoidal formulations will replace currently used formulas based on the spherical or even planar approximation of the inner boundary of the topographical masses. Besides the high accuracy of the GPS positions, the ellipsoidal formulas for the TP and TPG suffer from smaller approximation errors than the planar and spherical formulas. The remaining errors are related to topographical data (representing the continuous 2D height function by discrete values and approximating the unknown 3D mass density function).

In geodesy, the TP and TPG play an important role in the reduction of gravity data. Gravity data are traditionally collected over the land (ground gravity), more recently using aircraft (airborne gravity) and from satellites (satellite gravity). These data represent the Earth's gravity field in different

spatial resolutions: ground data contain all frequencies up to the noise level of gravimeters, airborne data are usually limited to a certain frequency band due to complex flight dynamics, and satellite data represent merely the long-frequency component due to the attenuation of the gravity field in the orbits of artificial satellites (usually few 100 km above ground). Thus, frequency specifications of particular gravity data are very important for selecting the proper approach and input data for evaluation of the TP and TPG.

A spatial (integral) representation of the TP based on the ellipsoidal approximation of the inner boundary of the topographical masses and the ellipsoidal coordinate system is presented in Sect. 2. A corresponding spatial formula for the TPG is then derived in Sect. 3. These formulas can directly be used for a local numerical evaluation of the TP and TPG using discrete description of the height function in the form of an ellipsoidal digital elevation model (EDEM). An ellipsoidal harmonic elevation model (EHEM) of the height function is used in Sect. 4 for the formulation of the spectral (series) formula for the TP. While the discrete values of the height function are now available globally due to the Shuttle Radar Topography Mission, SRTM (February 2000), with the exception of the polar caps and inland water, the ellipsoidal harmonic coefficients must be computed by ellipsoidal harmonic analysis of the ellipsoidal height function. Numerical values of the terrain potential and its vertical gradient obtained over a test area in the Canadian Rocky Mountains are presented in Sect. 5 and conclusions can be found in Sect. 6.

2 Gravitational potential of the topographical masses

Let $\mathbb{E}^3$ be a 3D Euclidean space with the Cartesian orthonormal right-handed coordinate system (X, Y, Z) and the associated unit base vectors $(\mathbf{e}_x, \mathbf{e}_y, \mathbf{e}_z)$. Let the origin of this coordinate system be at the centre of the Earth's mass, its Z-axis coinciding with the mean position of the Earth's rotational axis and its X-axis lying in the mean Greenwich meridian plane. The position of an arbitrary point in $\mathbb{E}^3$ can be defined through the geocentric radius vector $\mathbf{r} \in \mathbb{R}^3$

$$\mathbf{r} = \begin{bmatrix} \mathbf{e}_x & \mathbf{e}_y & \mathbf{e}_z \end{bmatrix} \begin{bmatrix} X & Y & Z \end{bmatrix}^T . \tag{1}$$

The two-parametric Gauss surface normal coordinates (L, B, H) are usually defined in terms of their transformation into the Cartesian system

$$\begin{aligned} X(L, B, H) &= [N(B) + H(L, B)] \cos B \cos L , \\ Y(L, B, H) &= [N(B) + H(L, B)] \cos B \sin L , \\ Z(L, B, H) &= [N(B)(1 - E^2) + H(L, B)] \sin B . \end{aligned} \tag{2}$$

The ellipsoidal longitude L, ellipsoidal latitude B and ellipsoidal height H can directly be derived from Cartesian coordinates obtainable via GPS. The ellipsoidal height function H refers the topographical surface to the surface of the geocentric biaxial ellipsoid used in geodesy as a reference body for geometric and gravity field applications. The shape and size of the geocentric reference ellipsoid are usually defined by

values of the major semi-axis A and the first numerical eccentricity E. The ellipsoidal prime vertical radius of curvature reads

$$N(B) = \frac{A}{\left(1 - E^2 \sin^2 B\right)^{1/2}} , \tag{3}$$

and the ellipsoidal meridian radius of curvature is

$$M(B) = \frac{A(1 - E^2)}{\left(1 - E^2 \sin^2 B\right)^{3/2}} . \tag{4}$$

The currently accepted values of A and E can be found, among other geodetic constants, in the Geodetic Reference System 1980, GRS80 (Moritz 1984).

Using the binomial expansion

$$(1 - x)^{-1/2} = 1 + \frac{1}{2} x + \frac{3}{8} x^2 + \cdots , \tag{5}$$

that can successfully be truncated for $|x| \ll 1$, both principal radii of curvature can be written as

$$N(B) = A\left(1 + \frac{1}{2} E^2 \sin^2 B\right) + \mathcal{O}(E^4) , \tag{6}$$

and

$$M(B) = A\left(1 + \frac{3}{2} E^2 \sin^2 B - E^2\right) + \mathcal{O}(E^4) . \tag{7}$$

where $\mathcal{O}$ stands for the Landau symbol showing as an argument, the power of the first omitted term in the series. The accuracy of E^2, which satisfies common accuracy requirements in geodesy, will be maintained throughout the following derivations. The two arguments of the height function H (ellipsoidal longitude L and ellipsoidal latitude B) as well as the argument of the radii of curvature N and M (ellipsoidal latitude B) are omitted in the following derivations to keep the expressions relatively simple. This means that for example the height of the computation point is abbreviated as $H(L, B) = H$ and the height of the integration point as $H(L^*, B^*) = H^*$. The geometry of the problem can be found in Fig. 1.

The TP can be computed by using the integral over the complete volume of the topographical masses. In Gauss ellipsoidal coordinates and for the computation point on the topography, it takes the form

$$V(L, B, H) = G \int_0^{2\pi} \int_{-\pi/2}^{\pi/2} \int_{\xi=0}^{H^*} \frac{\varrho(L^*, B^*, \xi)}{\mathcal{L}(L, B, H, L^*, B^*, \xi)}$$
$$\times (N^* + \xi)(M^* + \xi) \, d\xi \, \cos B^* dB^* \, dL^* , \tag{8}$$

where ϱ is the mass density function of the topographical masses, G is the universal gravitational constant and $\mathcal{L}$ is the Euclidean distance between the computation and integration points that can be conveniently evaluated from the Cartesian coordinates, see Eq. (2),

$$\begin{aligned} \mathcal{L}(L, &B, H, L^*, B^*, \xi) \\ &= \Big\{ [X(L, B, H) - X(L^*, B^*, \xi)]^2 \\ &\quad + [Y(L, B, H) - Y(L^*, B^*, \xi)]^2 \\ &\quad + [Z(L, B, H) - Z(L^*, B^*, \xi)]^2 \Big\}^{1/2} . \end{aligned} \tag{9}$$
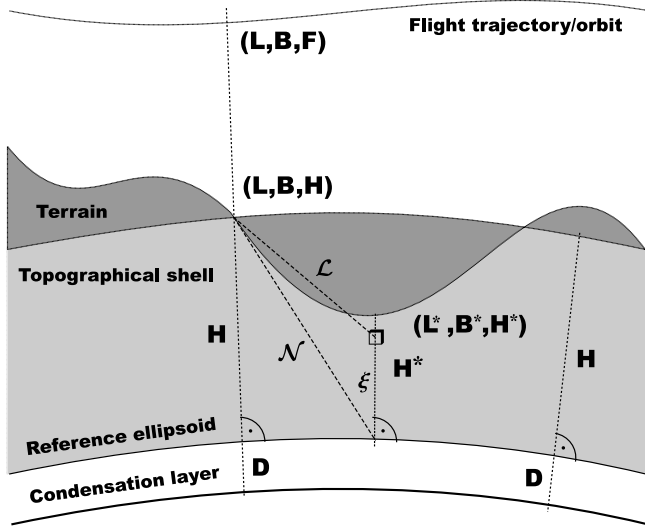
Fig. 1 Ellipsoidal geometry of topographical masses

In the above equations, the ellipsoidal coordinates with the asterisk, i.e. (L^*, B^*, ξ), define the position of an integrated infinitesimal volume, while the ellipsoidal coordinates without the asterisk, i.e. (L, B, H), define the position of the computation point (also see Fig. 1). The parameter ξ stands for the integration variable with the parameters L^* and B^* that are omitted. This notation also applies to the following expressions. Finally, the abbreviated notation is introduced for the full angle integration

$$\int_S dS = \int_0^{2\pi} \int_{-\pi/2}^{\pi/2} \cos B^* \, dB^* \, dL^* .$$

The TP in Eq. (8) is evaluated using available topographical data, namely discrete values of the height function H given on a regular grid in the EDEM and/or a set of coefficients in the EHEM. Since neither the 2D height function H nor the 3D mass density ϱ are known continuously, an appropriate form of the 3D integral must be found that reflects both the available form of input data and the required spatial resolution. Assuming, for simplicity, a constant mass density of the topographical masses, the innermost integral in Eq. (8) can be evaluated analytically. The relative error of this approximation, reaching up to 10%, can further be decreased by using a laterally-varying mass density, see e.g. Huang et al. (2001). Since this manuscript only deals with the geometry of the topographical masses and the laterally-varying density represents another approximation, only the constant mass density is used.

The volume integral in Eq. (8) is replaced by the surface integral that can be split into the three sub-integrals

$$\int_{\xi=0}^{H^*} \frac{1}{\mathcal{L}(L, B, H, L^*, B^*, \xi)} \left(N^* + \xi\right) \left(M^* + \xi\right) d\xi$$

$$= N^* M^* \int_{\xi=0}^{H^*} \frac{1}{\mathcal{L}(L, B, H, L^*, B^*, \xi)} \, d\xi$$

$$+ \left(N^* + M^*\right) \int_{\xi=0}^{H^*} \frac{\xi}{\mathcal{L}(L, B, H, L^*, B^*, \xi)} \, d\xi$$

$$+ \int_{\xi=0}^{H^*} \frac{\xi^2}{\mathcal{L}(L, B, H, L^*, B^*, \xi)} \, d\xi . \tag{10}$$

The three integrals in Eq. (10) have analytical solutions, which are derived in Appendix A

$$\int_{\xi=0}^{H^*} \frac{1}{\mathcal{L}(L, B, H, L^*, B^*, \xi)} \left(N^* + \xi\right) \left(M^* + \xi\right) d\xi$$

$$= A^2 \frac{1 - E^2}{\left(1 - E^2 \sin^2 B^*\right)^2} \mathcal{K}_1(L, B, H, L^*, B^*, H^*)$$

$$+ A \frac{2 - E^2 \left(1 + \sin^2 B^*\right)}{\left(1 - E^2 \sin^2 B^*\right)^{3/2}} \mathcal{K}_2(L, B, H, L^*, B^*, H^*)$$

$$+ \mathcal{K}_3(L, B, H, L^*, B^*, H^*) . \tag{11}$$

Substituting Eq. (11) into Eq. (8) yields the TP in the form

$$V(L, B, H) = G\varrho \, A^2 \int_S \mathcal{K}_1(L, B, H, L^*, B^*, H^*)$$

$$\times \frac{1 - E^2}{\left(1 - E^2 \sin^2 B^*\right)^2} \, dS$$

$$+ G\varrho \, A \int_S \mathcal{K}_2(L, B, H, L^*, B^*, H^*)$$

$$\times \frac{2 - E^2 \left(1 + \sin^2 B^*\right)}{\left(1 - E^2 \sin^2 B^*\right)^{3/2}} \, dS$$

$$+ G\varrho \int_S \mathcal{K}_3(L, B, H, L^*, B^*, H^*) dS . \tag{12}$$

Finally, the TP can be written as the sum

$$V(L, B, H) = V^s(L, B, H) + V^e(L, B, H) , \tag{13}$$

of the spherical TP

$$V^s(L, B, H)$$

$$= G\varrho \int_S \Big[A^2 \, \mathcal{K}_1(L, B, H, L^*, B^*, H^*)$$

$$+ 2A \, \mathcal{K}_2(L, B, H, L^*, B^*, H^*)$$

$$+ \mathcal{K}_3(L, B, H, L^*, B^*, H^*) \Big] \, dS , \tag{14}$$

and the ellipsoidal correction to the spherical TP

$$V^e(L, B, H) = G\varrho E^2 \int_S \Big[A^2 \mathcal{K}_1(L, B, H, L^*, B^*, H^*)$$

$$+ A\mathcal{K}_2(L, B, H, L^*, B^*, H^*) \Big]$$

$$\times \left(2 \sin^2 B^* - 1\right) dS + \mathcal{O}(E^4). \tag{15}$$

The expression in Eq. (14) is fully consistent with spherical formulas previously derived by, e.g., Martinec and Vaníček (1994). Equations (14) and (15) can be numerically evaluated by a quadrature approach using as input data discrete values of the EDEM or by a series expansion using the EHEM. Note that Eq. (15) has only the accuracy of E^2 while the integral in Eq. (14) contains no approximation. The terms starting with E^4 are usually neglected in ellipsoidal expressions due to their negligible magnitude. For the sphere

$$\lim_{E \to 0} V^e(L, B, H) = 0 \,, \tag{16}$$

and one gets the ordinary spherical approximation of the topographical potential, see e.g. Novák (2000).

Assuming the computation point on the topography (e.g., for the reduction of ground gravity data), the integrals in Eqs. (14) and (15) are both singular at the computation point. Numerical aspects of the spherical Newtonian integrals such as stability and singularity were studied by Martinec (1998) with conclusions also applicable to the above integrals: by discretizing the integrals using the average values of the ellipsoidal height function, the singularities can be removed and solved for independently. The integration limits for the direction (L^*, B^*) represent the reference ellipsoid and the corresponding point at the topography with the elevation H^*. This integration domain is usually split into two sub-domains: the first being limited by the reference ellipsoid and the elevation of the computation point (this corresponds to a topographical shell of constant thickness H), and the second being limited by the elevation of the computation point and the elevation of the topography in the corresponding direction, i.e.

$$\int_{\xi=0}^{H^*} \mathrm{d}\xi = \int_{\xi=0}^{H} \mathrm{d}\xi + \int_{\xi=H}^{H^*} \mathrm{d}\xi \,. \tag{17}$$

The former potential represented by the first integral on the right-hand-side of Eq. (17) is the singularity of the integral in Eq. (8). It is generated by the topographical shell bounded by the reference ellipsoid and a surface with the constant height H above the reference ellipsoid. Its approximate solution can be derived with high level of accuracy as the difference of potentials of two homogeneous ellipsoids (MacMillan 1958). The corresponding counterpart for the planar approximation of topography is the potential of the so-called Bouguer plate (a homogeneous infinite planar slab) and for the spherical approximation, the potential of the homogeneous spherical shell. The singularity of the TP in Eq. (14) corresponds to the potential of the homogeneous spherical shell (Vaníček et al. 2001). The singularity of the ellipsoidal correction in Eq. (15) is introduced in Appendix B. The singularities are not evaluated numerically due to their compensation by condensed topography.

The latter potential, i.e. the second integral on the right-hand-side of Eq. (17), represents the potential of terrain, i.e. topographical mass redundancy or deficiency with respect to the homogeneous shell, that can only be evaluated numerically. Combining Eqs. (14) and (15) in a single quadrature

formula yields the terrain potential (i.e., that of the topography residual to the Bouguer shell)

$$\delta V(L, B, H) = G\varrho \sum_j \Delta S_j \left\{ A^2 \mathcal{K}_1(L, B, H, L_j, B_j, H_j) \right.$$
$$\times \left[1 + E^2 \left(2 \sin^2 B_j - 1 \right) \right]$$
$$+ A\mathcal{K}_2(L, B, H, L_j, B_j, H_j)$$
$$\times \left[2 + E^2 \left(2 \sin^2 B_j - 1 \right) \right]$$
$$\left. + \mathcal{K}_3(L, B, H, L_j, B_j, H_j) \right\} + \mathcal{O}(E^4) \,. \tag{18}$$

The spectral formulation of Eq. (18) will be introduced in Sect. 4. Although Eq. (18) is not singular, numerical instabilities remain and results are sensitive to the description of the topography close to the computation point, especially in mountainous areas. These complications are also shared by the planar and spherical formulas. The summation in Eq. (18) is evaluated over discrete values of the kernel functions $\mathcal{K}$ that correspond to the computation point (L, B, H) and the centre of the j-th geographical cell defined in terms of its centre (L_j, B_j) and its average ellipsoidal height H_j. These data are stored in the EDEM on a regular grid in terms of ellipsoidal coordinates. The weight ΔS, in Eq. (18), for the j-th parallel in case of the uniform resolution ΔB in latitude and ΔL in longitude is

$$\Delta S_j = \cos B_j \, \Delta B \, \Delta L \,. \tag{19}$$

There are many possible approaches for numerical evaluation of the surface integrals. The scheme used in Eq. (18) is often used in geodesy providing satisfactory accuracy with respect to the quality of integrated height data. However, investigations on the most suitable numerical evaluation of the 2D integrals are out of the scope of this article.

Equation (18) can be applied for the reduction of ground gravity data, for the TP generated by the topographical masses in the vicinity of the gravity station, since the discrete heights from the EDEM provide the necessary high-frequency signal. Currently, gravity data observed at low-altitude flying platforms (airborne gravimetry), derived from satellite dynamics (perturbation theory) or specific satellite data (gravity-dedicated satellite missions) becomes increasingly important. Numerical values of the TP generated by the close topography (high-frequency signal) become smaller with the increasing elevation of the computation point from the Earth's surface. In contrast to the ground data, the low-frequency component of the TP generated mainly by distant topographical masses becomes more important. The TP at the point with the elevation $F > H$ above the reference ellipsoid reads

$$V(L, B, F) = G \int_S \int_{\xi=0}^{H^*} \frac{\varrho(L^*, B^*, \xi)}{\mathcal{L}(L, B, F, L^*, B^*, \xi)}$$
$$\times \left(N^* + \xi \right) \left(M^* + \xi \right) \mathrm{d}\xi \, \mathrm{d}S \,. \tag{20}$$

As can be seen from Eq. (20), the formulation of the integral does not differ significantly from Eq. (8). However, its numerical values can differ very much depending upon the

value of the elevation F. The important difference is that the integral in Eq. (20) is not singular. It is also less sensitive to variations of the height function in the vicinity of the point at the topography with the coordinates (L, B, H). The spectral approach discussed in Sect. 4 allows then for adjustment of the frequency content of the TP according to the gravity data to be used.

Due to its large values, the TP is usually counterbalanced by the gravitational potential of a simple layer located on or inside the reference ellipsoid. Note that the spheroidal Bruns transform (Grafarend et al. 1999) is considered in this article. The generalized Helmert approach (Heck 2003) is outlined with the layer being located in the constant depth D below the surface of the reference ellipsoid. Such a gravitational potential, abbreviated as the potential of the condensed topography (CTP), can be written as

$$V^c(L, B, H) = G \int_S \frac{\sigma(L^*, B^*)}{\mathcal{L}(L, B, H, L^*, B^*, D^*)}$$
$$\times (N^* - D) (M^* - D) \, dS, \qquad (21)$$

with the surface mass density of the layer σ. Assuming $D = 0$, then

$$V^c(L, B, H) = G \int_S \frac{\sigma(L^*, B^*)}{\mathcal{N}(L, B, H, L^*, B^*)} N^* M^* \, dS. \quad (22)$$

The distance function $\mathcal{N}$ is defined by Eq. (53). Assuming mass-conservation compensation, i.e. the mass of the Earth (zero-degree harmonic in the harmonic expansion of the geopotential) is not affected, the surface mass density can be derived from

$$\int_S \sigma(L^*, B^*) \, N^* \, M^* \, dS = \int_S \int_{\xi=0}^{H^*} \varrho(L^*, B^*, \xi) (N^* + \xi)$$
$$(M^* + \xi) \, d\xi \, dS. \quad (23)$$

Assuming again, the constant mass density of the topographical masses, the surface mass density is

$$\sigma(L^*, B^*) = \frac{\varrho}{N^* M^*} \int_{\xi=0}^{H^*} (N^* + \xi) (M^* + \xi) \, d\xi, \quad (24)$$

and

$$\sigma(L^*, B^*) = \varrho \, H^* \left[1 + \frac{H^*}{2} \frac{N^* + M^*}{N^* M^*} + \frac{H^{*2}}{3} \frac{1}{N^* M^*} \right]. \quad (25)$$

For the sphere

$$\lim_{E \to 0} \sigma(L^*, B^*) = \varrho \, H^* \left(1 + \frac{H^*}{A} + \frac{H^{*2}}{3A^2} \right), \quad (26)$$

that yields the form of the spherical approximation of the mass density σ, see Martinec (1998, Eq. 3.20).

Substituting the surface density in Eq. (25) into Eq. (22) yields the CTP in the form

$$V^c(L, B, H) = G\varrho \int_S \left[N^*M^* + \frac{H^*}{2} (N^* + M^*) + \frac{H^{*2}}{3} \right]$$
$$\times \frac{H^*}{\mathcal{N}(L, B, H, L^*, B^*)} \, dS. \quad (27)$$

Substituting for the ellipsoidal radii of curvature (Eqs. 3 and 4), the CTP can be decomposed similar to the TP, see Eqs. (14) and (15), into the spherical CTP

$$V^{cs}(L, B, H) = GA^2 \int_S \frac{\sigma^s(L^*, B^*)}{\mathcal{N}(L, B, H, L^*, B^*)} \, dS, \quad (28)$$

with the surface density

$$\sigma^s(L^*, B^*) = \varrho \, H^* \left(1 + \frac{H^*}{A} + \frac{H^{*2}}{3A^2} \right), \quad (29)$$

and the ellipsoidal correction to the spherical CTP

$$V^{ce}(L, B, H) = GA^2 E^2 \int_S \frac{\sigma^e(L^*, B^*)}{\mathcal{N}(L, B, H, L^*, B^*)}$$
$$\times (2 \sin^2 B^* - 1) \, dS + \mathcal{O}(E^4), \quad (30)$$

with the surface density

$$\sigma^e(L^*, B^*) = \varrho \, H^* \left(1 + \frac{H^*}{2A} \right). \quad (31)$$

Again for the sphere

$$\lim_{E \to 0} V^{ce}(L, B, H) = 0, \quad (32)$$

and the spherical approximation of the CTP, see Eq. (28), is obtained. Although there is no singularity involved in these integrals, the CTP is evaluated in a way similar to the TP, i.e. the integral in Eq. (24) is split into two components: the first one corresponds to the condensed topographical shell and the second one to the condensed terrain. This can be easily done by applying the separation in Eq. (17) to the integral in Eq. (24). The main reason for this practice is the similarity of the potential of the topographical masses with the potential of the condensed topographical masses. In the spherical approximation (Martinec 1998), the potential of the spherical shell cancels with the potential of its condensed counterpart (at the computation point on or above the topography and for the mass-conservation compensation). In the ellipsoidal approximation discussed here, the shell contribution of the ellipsoidal corrections must also be considered, see Eqs. (15), (30) and Appendix B.

3 Vertical gradient of the topographical potential

Assuming that gravity rather than the potential can be observed, it is also interesting to investigate the gravitational effect of the topographical masses. Although the gravitation (vector) can be derived from the corresponding potential as

its gradient, only the vertical component is generally observable at the ground level.

The TPG is defined (sign convention as used for gravity reduction) as

$$\Gamma(L, B, H) = \frac{\partial}{\partial H} V(L, B, H).$$ (33)

The directional derivative of the TP, see Eq. (8), is taken with respect to the ellipsoidal normal. However, the measured component of ground gravity relates to the direction of the local plumbline and a corresponding correction should be taken into the account. Since its size, which depends on the magnitude of the deflection of verticals, is rather small (Novák 2000), this correction is usually neglected. Substituting for the TP from Eq. (8) yields the TPG in the form

$$\Gamma(L, B, H)$$
$$= G\varrho \int\limits_{S} \int\limits_{\xi=0}^{H^*}$$
$$\times \left[\frac{\partial}{\partial H} \frac{(N^* + \xi) (M^* + \xi)}{\mathcal{L}(L, B, H, L^*, B^*, \xi)} \right] d\xi \, dS.$$ (34)

Similarly to the TP, the innermost integral in Eq. (34) can also be evaluated analytically. Generally, the integral can be derived as follows

$$\int\limits_{\xi=0}^{H^*} \left[\frac{\partial}{\partial H} \frac{(N^* + \xi) (M^* + \xi)}{\mathcal{L}(L, B, H, L^*, B^*, \xi)} \right] d\xi$$
$$= A^2 \frac{1 - E^2}{\left(1 - E^2 \sin^2 B^*\right)^2} \, \mathcal{P}_1(L, B, H, L^*, B^*, H^*)$$
$$+ A \frac{2 - E^2 \left(1 + \sin^2 B^*\right)}{\left(1 - E^2 \sin^2 B^*\right)^{3/2}} \, \mathcal{P}_2(L, B, H, L^*, B^*, H^*)$$
$$+ \mathcal{P}_3(L, B, H, L^*, B^*, H^*).$$ (35)

The derivation of the functions $\mathcal{P}$ is shown in Appendix C. Similar to the TP, see Eqs. (14) and (15), the TPG can also be expressed as a sum of the spherical TPG

$$\Gamma^s(L, B, H) = G\varrho \int\limits_{S} \left[A^2 \, \mathcal{P}_1(L, B, H, L^*, B^*, H^*) \right.$$
$$+ 2A \, \mathcal{P}_2(L, B, H, L^*, B^*, H^*)$$
$$\left. + \mathcal{P}_3(L, B, H, L^*, B^*, H^*) \right] dS,$$ (36)

and the ellipsoidal correction to the spherical TPG

$$\Gamma^e(L, B, H) = G\varrho \, E^2 \int\limits_{S} \left[A^2 \, \mathcal{P}_1(L, B, H, L^*, B^*, H^*) \right.$$
$$\left. + A \, \mathcal{P}_2(L, B, H, L^*, B^*, H^*) \right]$$
$$\times \left(2 \sin^2 B^* - 1\right) dS + \mathcal{O}(E^4).$$ (37)

Due to the singularity of the integral in Eq. (34), the integration limits for ξ are treated in a way similar to the TP in Sect. 2, i.e. the effect of the Bouguer shell and the terrain

are evaluated independently. For the numerical evaluation of the terrain effect corresponding to the terrain potential in Eq. (18), the following quadrature formula can be applied

$$\delta\Gamma(L, B, H) = G\varrho \sum_{j} \Delta S_j \left\{ A^2 \mathcal{P}_1(L, B, H, L_j, B_j, H_j) \right.$$
$$\times \left[1 + E^2 \left(2 \sin^2 B_j - 1 \right) \right]$$
$$+ A \, \mathcal{P}_2(L, B, H, L_j, B_j, H_j)$$
$$\times \left[2 + E^2 \left(2 \sin^2 B_j - 1 \right) \right]$$
$$\left. + \mathcal{P}_3(L, B, H, L_j, B_j, H_j) \right\} + \mathcal{O}(E^4).$$ (38)

The values of the TPG can be reduced using the gravitational effect of the single layer introduced in Sect. 3. The directional derivative is then applied on the CTP

$$\Gamma^c(L, B, H) = \frac{\partial}{\partial H} V^c(L, B, H),$$ (39)

called the gradient of the CTP (CTPG). Its spherical component has the form, see Eq. (28),

$$\Gamma^{cs}(L, B, H)$$
$$= G A^2 \int\limits_{S} \sigma^s(L^*, B^*) \, \mathcal{W}(L, B, H, L^*, B^*) \, dS,$$ (40)

and the corresponding ellipsoidal correction is, see Eq. (30),

$$\Gamma^{ce}(L, B, H) = G A^2 E^2 \int\limits_{S} \sigma^e(L^*, B^*) \mathcal{W}(L, B, H, L^*, B^*)$$
$$\times \left(2 \sin^2 B^* - 1\right) dS + \mathcal{O}(E^4).$$ (41)

The integration kernel $\mathcal{W}$ is defined as, see Eq. (61) for $\xi = 0$,

$$\mathcal{W}(L, B, H, L^*, B^*) = \frac{\partial}{\partial H} \frac{1}{\mathcal{N}(L, B, H, L^*, B^*)}.$$ (42)

4 Spectral form of the topographical potential

The discrete integration (summation) in Eqs. (18) and (38), applied in global computations of the TP or TPG, represents a demanding numerical problem. Instead of using the discrete height data, the spectral representation of the global height function H in terms of the set of coefficients in the EHEM is a more convenient choice for the input data. Moreover, the spectral representation allows for tuning the frequency content of resulting values that is very important for reduction of frequency-limited data. The approach is similar to the spherical harmonic representations of the topographical potential and its vertical gradient (Novák et al. 2003). However, the approach discussed in this section differs in the selection of base functions that reflect the shape of the reference ellipsoid.

The ellipsoidal height function H can be expanded into the harmonic series (Grafarend and Engels 1992, Eq. 2.7)

$$H(L, B) = \sum_{n=0}^{\infty} H_n(L, B, E),$$ (43)

of the zonal harmonics

$$H_n(L, B, E) = \sum_{m=0}^{n} H_{n,m} \, Z_{n,m}(L, B, E) \,. \tag{44}$$

The orthonormal base functions with respect to the reference ellipsoid with the eccentricity E read as

$$
\begin{aligned}
&Z_{n,m}(L, B, E) \\
&= \sqrt{\frac{1}{2} + \frac{1 - E^2}{4E} \, \ln \frac{1 + E}{1 - E}} \, \frac{\sqrt{2n + 1}}{\varepsilon_m} \sqrt{\frac{(n - m)!}{(n + m)!}} \\
&\quad \times \frac{1 - E^2 \sin^2 B}{\sqrt{1 - E^2}} \, (\cos mL + \sin mL) \, P_{n,m}(\sin B) \,,
\end{aligned}
\tag{45}
$$

$$\varepsilon_m = \begin{cases} 1 & \text{if } m = 0 \,, \\ \sqrt{\frac{1}{2}} & \text{otherwise} \,, \end{cases} \tag{46}$$

with the degree n, order m and associated Legendre functions $P_{n,m}$. The TP based on the spectral representation of H in Eq. (43) will contain only frequencies corresponding to the maximum degree of the EHEM. If required, the missing high-frequency signal can be added using local integration. The integration radius in Eq. (18) should be selected with respect to the highest available harmonic degree in Eq. (43) and the height functions should be reduced similar to gravity data used for their inversion to the potential in the remove-compute-restore technique.

In this section, the spectral form of the TP is derived. Since such a representation allows for adjustment of its frequency content, this approach is particularly suitable for reduction of airborne and satellite gravity data, i.e. the computation point is located at the height F above the reference ellipsoid. Moreover, it is assumed that the point is located outside the Brillouin sphere. A similar approach can be used for spectral formulas of the CTP, as well as their vertical gradients. The methodology follows derivations by Novák et al. (2001), where the spherical approximation was considered. The first step consists of deriving such a representation of the TP that could be replaced by a series of the ellipsoidal harmonics in Eq. (44). The integration kernels in Eq. (12) are then replaced by the convolution of ellipsoidal heights with new functions. The kernel functions $\mathcal{K}$ are expanded into the Taylor series of the ellipsoidal height function at the direction (B, L), see Fig. 1,

$$
\begin{aligned}
&\mathcal{K}_i(L, B, F, L^*, B^*, H^*) = \mathcal{K}_i(L, B, F, L^*, B^*, H) \\
&\quad + \sum_{n=1}^{\infty} \frac{1}{n!} \left. \frac{\partial^n \mathcal{K}_i(L, B, F, L^*, B^*, H^*)}{\partial H^{*n}} \right|_{H^* = H} \\
&\quad \times \left(H^* - H \right)^n \,, \quad i = \{1, 2, 3\} \,.
\end{aligned}
\tag{47}
$$

Similar series expansions of the Newtonian kernels were discussed for case of the spherical approximation by Martinec (1998). First-order derivatives of the kernel functions $\mathcal{K}$ are trivial, see their definitions in Eqs. (54)–(56); second- and third-order derivatives can be found in Appendix D. The TP up to E^2 has the spatial form

$$
\begin{aligned}
V(L, B, F) = G\varrho \int_S & \left\{ A^2 \, \mathcal{K}_1(L, B, F, L^*, B^*, H^*) \right. \\
& \times \left[1 + E^2 \left(2 \sin^2 B^* - 1 \right) \right] \\
& + A \, \mathcal{K}_2(L, B, F, L^*, B^*, H^*) \\
& \times \left[2 + E^2 \left(2 \sin^2 B^* - 1 \right) \right] \\
& \left. + \mathcal{K}_3(L, B, F, L^*, B^*, H^*) \right\} \, \mathrm{d}S \,,
\end{aligned}
\tag{48}
$$

where the spherical potential and its ellipsoidal correction are combined. Substituting the kernel functions by the series in Eq. (47) and the height function by the series in Eq. (43), the spectral TP can be expressed as

$$
\begin{aligned}
V(L, B, F) = G\varrho & \left[A^2 \, \mathcal{J}_1^{(0)}(L, B, F, H) \right. \\
& \left. + A \mathcal{J}_2^{(0)}(L, B, F, H) + \mathcal{J}_3^{(0)}(L, B, F, H) \right] \\
& + G\varrho \sum_{i=1}^{\infty} \sum_{n=0}^{\infty} \sum_{m=0}^{n} H_{n,m}^i \left[A^2 \, \mathcal{J}_{1,n,m}^{(i)}(L, B, F, H) \right. \\
& \left. + A \mathcal{J}_{2,n,m}^{(i)}(L, B, F, H) + \mathcal{J}_{3,n,m}^{(i)}(L, B, F, H) \right] \,.
\end{aligned}
\tag{49}
$$

The formulation of the functions $\mathcal{J}$ is outlined in Appendix E. While the first term corresponds to the potential of the topographical shell, the second and third terms represent corrections due to deviations of the actual topographical masses from the shell (herein, the terrain). The important issue is the convergence (i.e. its rate and uniformity) of the series in Eq. (49) that would justify its truncation and leave corresponding omission errors negligibly small. However, the convergence is also of theoretical importance since Eq. (49) was obtained from Eq. (48) by replacing the order of integration and summation. This would apply for the computation point located inside the Brillouin sphere. This problem is not discussed in this article since the spectral approach is applied to frequency-limited data outside topographical masses. Numerical coefficients of the ellipsoidal height functions can be obtained for the i-th power via the ellipsoidal harmonic analysis (Grafarend and Engels 1993, Eq. 2.9) for $i = 1, 2, 3, \ldots$

$$
\begin{aligned}
H_{n,m}^i = \frac{1}{2\pi} & \left(\frac{1}{2E} \, \ln \frac{1 + E}{1 - E} + \frac{1}{1 - E^2} \right)^{-1} \\
& \times \int_S H^{*i} \, Z_{n,m}(L^*, B^*, E) \frac{1}{\left(1 - E^2 \sin^2 B^* \right)^2} \, \mathrm{d}S \,.
\end{aligned}
\tag{50}
$$

5 Numerical investigations

The spatial formulas in Sects. 2 and 3 were coded and evaluated numerically over a test area in the Canadian Rocky Mountains. This region is suitable for the numerical testing of the computations of the terrain effects due to its somewhat extreme topographical complexity. The 1×1 arcdeg computation area is bounded by the parallels of 50 and 51 arcdeg N, and by the meridians of 242 and 243 arcdeg E. The input
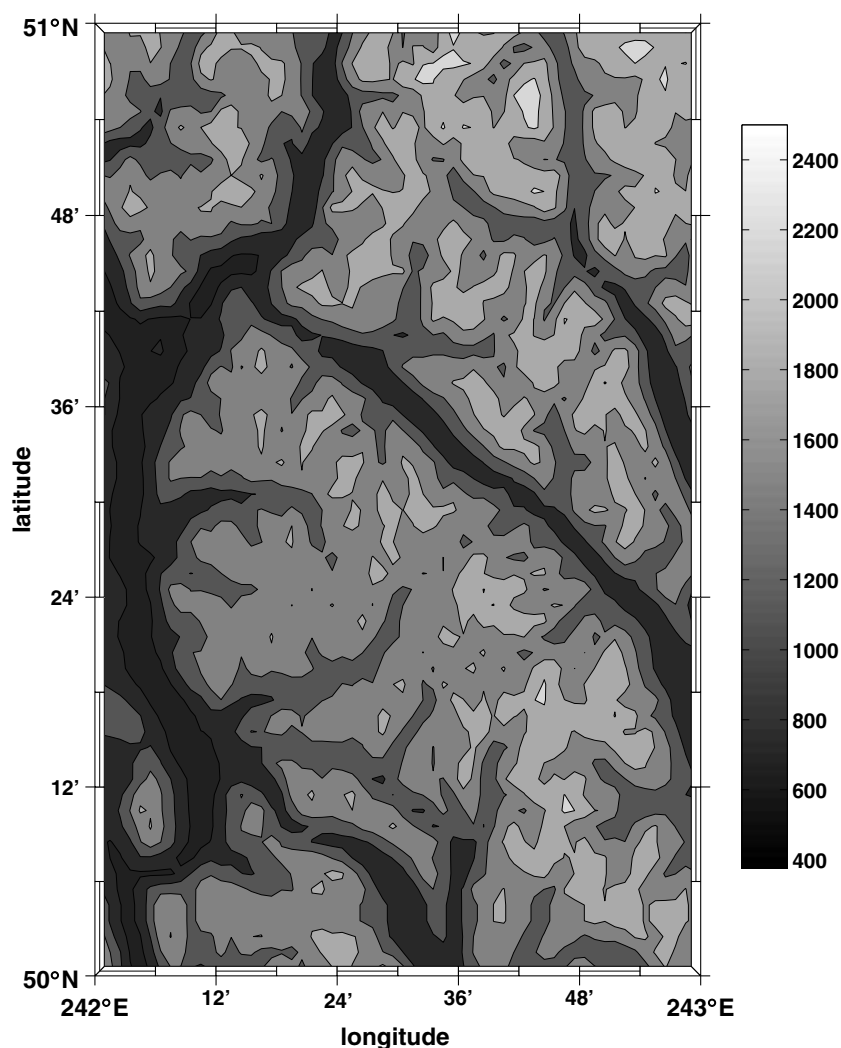
Fig. 2 Height function H in the test area (m)

elevation data represented by 3×3 arcsec (approximately 100×100 m) discrete values of the height function, H, were taken from the EDEM over the 3×5 arcdeg area bounded by the parallels of 49 and 52 arcdeg N, and by the meridians of 240 and 245 arcdeg E. These particular heights were generated from the local DEM using a regional geoid model. Large data area is considered in order to avoid edge effects in the results. The topography of the computation area is plotted in Fig. 2 and its statistical values are in Table 1.

Discrete values of the terrain potential δV, condensed terrain potential δV^c and their vertical gradients $\delta \Gamma$ and $\delta \Gamma^c$ were evaluated at the 1×1 arcmin grid, i.e. samples of 3,600 discrete values of the potential and its vertical gradient were computed using Eqs. (18) and (38). The integration domain was limited by the radius of 1 arcdeg (approximately 100 km). This means that the effect of terrain and its condensed counterpart within this radius around each computation point was computed that is consistent with practical computations when only the local topography is considered. The sample results

for the terrain potential are plotted in Fig. 3 (spherical terrain potential δV^s) and Fig. 4 (ellipsoidal terrain potential correction δV^e). The results of the corresponding vertical gradients are there in Fig. 5 (spherical terrain gradient $\delta \Gamma^s$) and Fig. 6 (ellipsoidal terrain gradient correction $\delta \Gamma^e$). Since the plots for the condensed terrain potential resemble those for the terrain potential, only its gradient is shown in Fig. 7 (spherical condensed terrain gradient $\delta \Gamma^{cs}$) and Fig. 8 (ellipsoidal condensed terrain gradient correction $\delta \Gamma^{ce}$).

The numerical results for the spherical terrain potential and its vertical gradient were successfully checked against values computed by the spherical formulas derived by Martinec and Vaníček (1994). It is also interesting to look at basic statistical values of the computed samples (Table 1). The ellipsoidal corrections in Table 1 represent the differences between the spherical and ellipsoidal formulations of the potentials and their vertical gradients. Thus, these values can be seen as a direct consequence of using the ellipsoidal model on the limited integration domain. Generally, the

Table 1 Statistics of input and output data for numerical tests in the Canadian Rocky Mountains

Function	Minimum	Maximum	Mean	Sigma	R.M.S.	Units
H	376.0	2743.0	1538.6	531.0	–	m
δV^s	−123.979	139.596	3.669	59.788	59.892	$m^2\ s^{-2}$
δV^e	−0.169	0.182	0.005	0.076	0.077	
δV^{cs}	−122.523	139.604	3.794	59.589	59.701	
δV^{ce}	−0.167	0.182	0.005	0.076	0.076	
$\delta \Gamma^s$	3.145	100.325	30.245	13.660	33.186	mGal
$\delta \Gamma^e$	0.004	0.118	0.039	0.018	0.042	
$\delta \Gamma^{cs}$	−94.077	92.083	4.492	29.287	29.626	
$\delta \Gamma^{ce}$	−0.110	0.111	0.006	0.037	0.038	
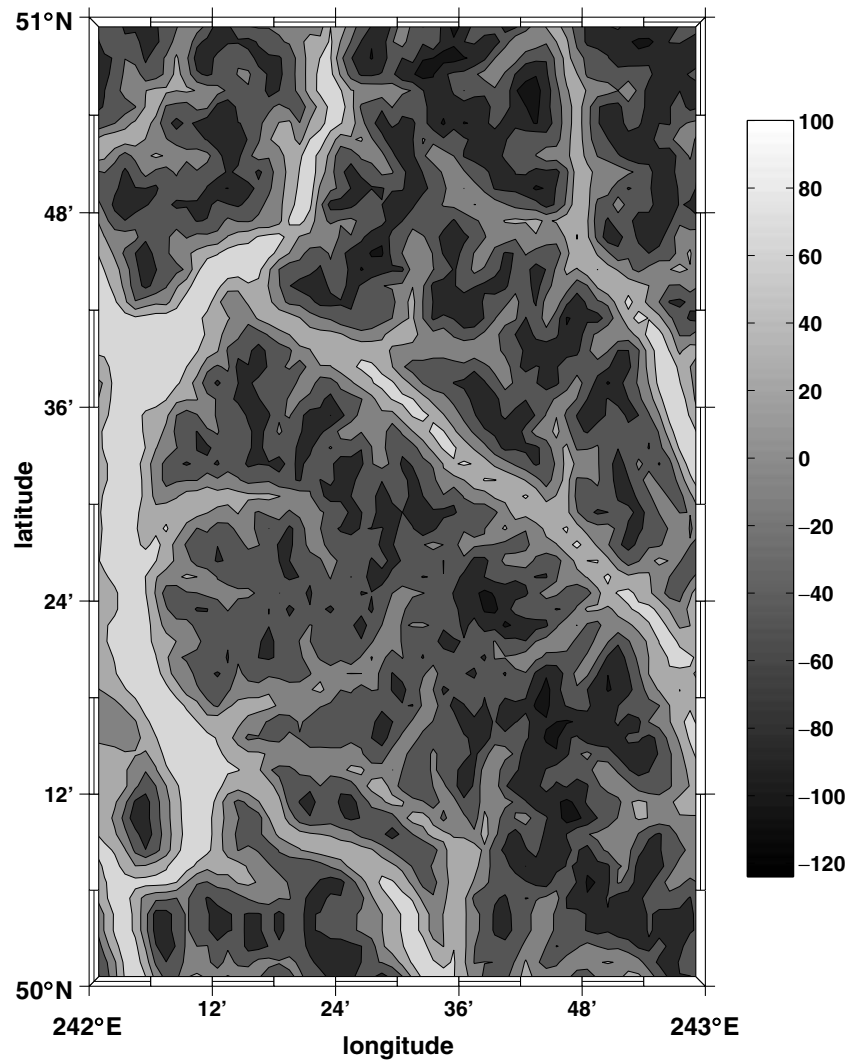
Fig. 3 Spherical terrain potential δV^s ($m^2\ s^{-2}$)

contribution of the ellipsoidal corrections is at the level of 10^{-3} of the spherical term that corresponds to the magnitude of ellipsoidal corrections in comparable computations based on integration (Lelgeman 1970). The terrain potential is well compensated by the single layer potential, in contrast to its gradient.

The evaluation of both the functions (TP and TPG) in the spatial domain represents a demanding numerical task. The local computation by the quadrature approach can be also replaced by the solution in the frequency domain using the fast Fourier transform (FFT), namely its 1D variety. Since the corresponding integrals are not of the convolutive type,
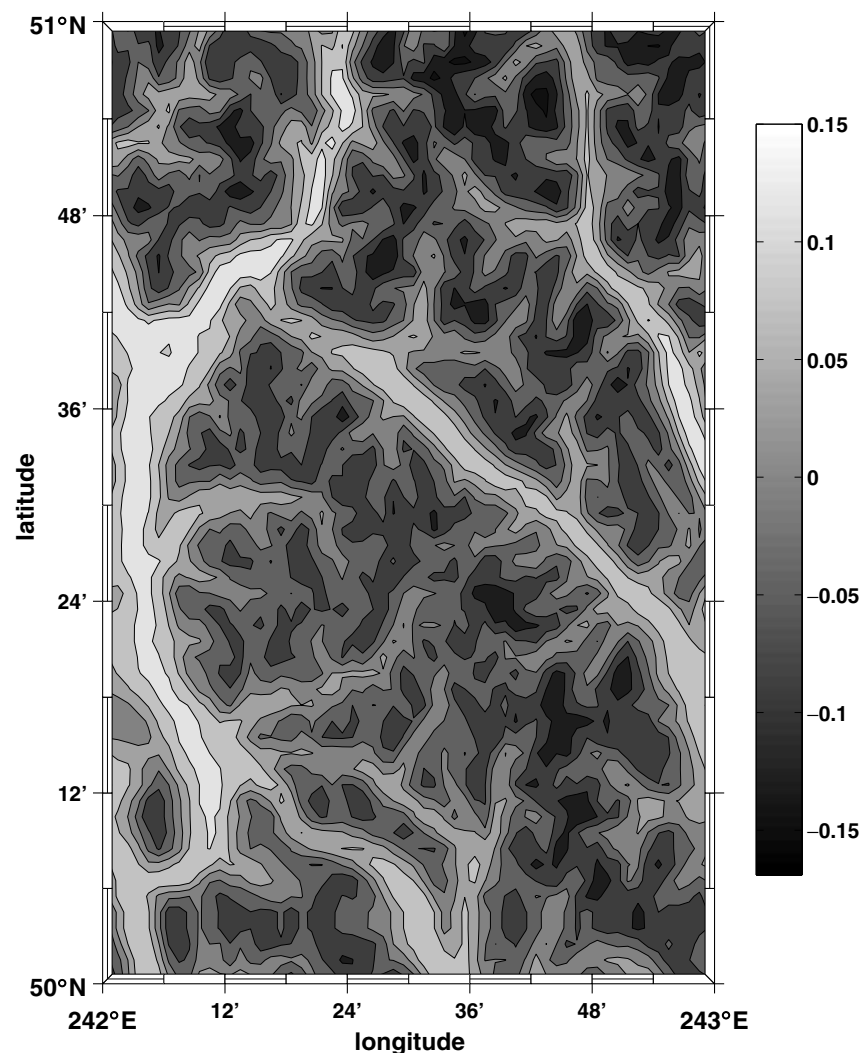
Fig. 4 Ellipsoidal correction to the spherical terrain potential δV^e (m^2 s^{-2})

an additional effort is required for getting their suitable form. The FFT provides generally the same results if applied consistently with the space-wise integration (Novák et al. 2001). However, in practice, the FFT usually operates on data across the entire area that may lead to different results. The choice of the numerical method is assumed to be outside the scope of this article and will not be discussed here any further.

A final remark concerns the integration kernels in Eqs. (11) and (35). In contrast to the spherical formulation, the integration kernels are functions of both the spherical distance and the azimuth. Figure 9 shows the behaviour of the integration kernels as a function of the distance for the primary directions south–north and east–west. The upper graph in Fig. 9 shows the kernel in Eq. (11) for the selected values of the parameters $H = 500$ m and $H^* = 1,000$ m. The lower graph in Fig. 9 applies to the integration kernel in Eq. (35) for the same values of H and H^*. At first glance, both functions behave in a similar fashion. The difference is in the scale on the vertical axes that reveals how much faster the kernel in Eq. (35) attenuates with increasing distance. There is also an

obvious difference between the values of the kernels for the two azimuths.

6 Conclusions

The gravitational potential of the topographical masses (TP) and its vertical gradient (TPG) have been formulated in terms of the GPS-based ellipsoidal coordinates (L, B, H). The spatial formula for the TP is represented by Eq. (12) and the spectral formula by Eq. (49). These formulas can be used independently or they can complement each other depending on the intended application. The spatial solution could be deployed for computation of the high-frequency components of the TP generated by the topographical masses in the vicinity of the computation point. These values are required for topographical reduction of ground gravity data used in geoid computations using the remove-compute-restore technique. The spectral solution is then suitable for the evaluation of the long-wavelength component of the TP up to the maximum
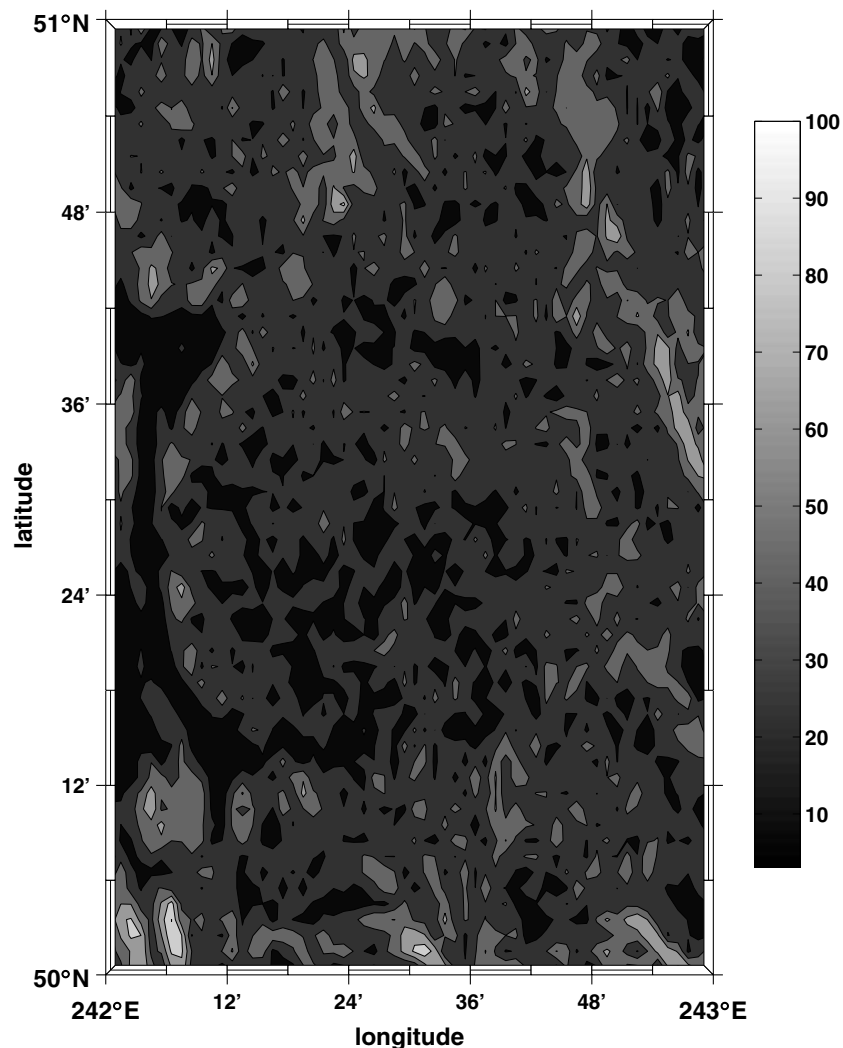
Fig. 5 Spherical terrain gradient $\delta\Gamma^s$ (mGal)

degree of the available EHEM. These values might also be interesting for the topographical reduction of gravity data derived from airborne and spaceborne sensors. The single-layer potential and its vertical gradient were used as an example for application of the ellipsoidal formalism in this area. The TPG and its vertical gradient CTPG were formulated using only the spatial form.

The new formulas take the advantage of the accurate GPS positioning of the topographical surface. In contrast to the planar and spherical formulas frequently used in geodesy for evaluation of the TP and TPG, the new formulas do not suffer from errors originating in the geometric approximation of the topographical masses, namely their inner boundary. This applies for the spheroidal Bruns transform with the reference ellipsoid as the inner boundary of the topographical masses. Although the magnitude of the ellipsoidal corrections to the TP and TPG might seem small and thus of a limited importance for practical calculations, one should not forget their additional advantages stemming from the use of coordinates that are directly observable with high level of accuracy

and represent the natural coordinate system for the reference ellipsoid. Although the computed values refer to one of the most complex topographical surfaces, the ellipsoidal corrections may affect the geoid at the centimetre level. Thus, they should not be neglected if the centimetre geoid is required.

Appendix A

Kernel functions $\mathcal{K}$

One can start the derivations with the distance function $\mathcal{L}$ between the computation point (L, B, H) and integration point (L^*, B^*, ξ), see Eq. (9). For its integration over the parameter ξ, see Eq. (10), the function $\mathcal{L}$ can be expressed as the polynomial

$$\mathcal{L}(L, B, H, L^*, B^*, \xi) = \left[\xi^2 + 2\,\mathcal{M}(L, B, H, L^*, B^*)\,\xi \right.$$
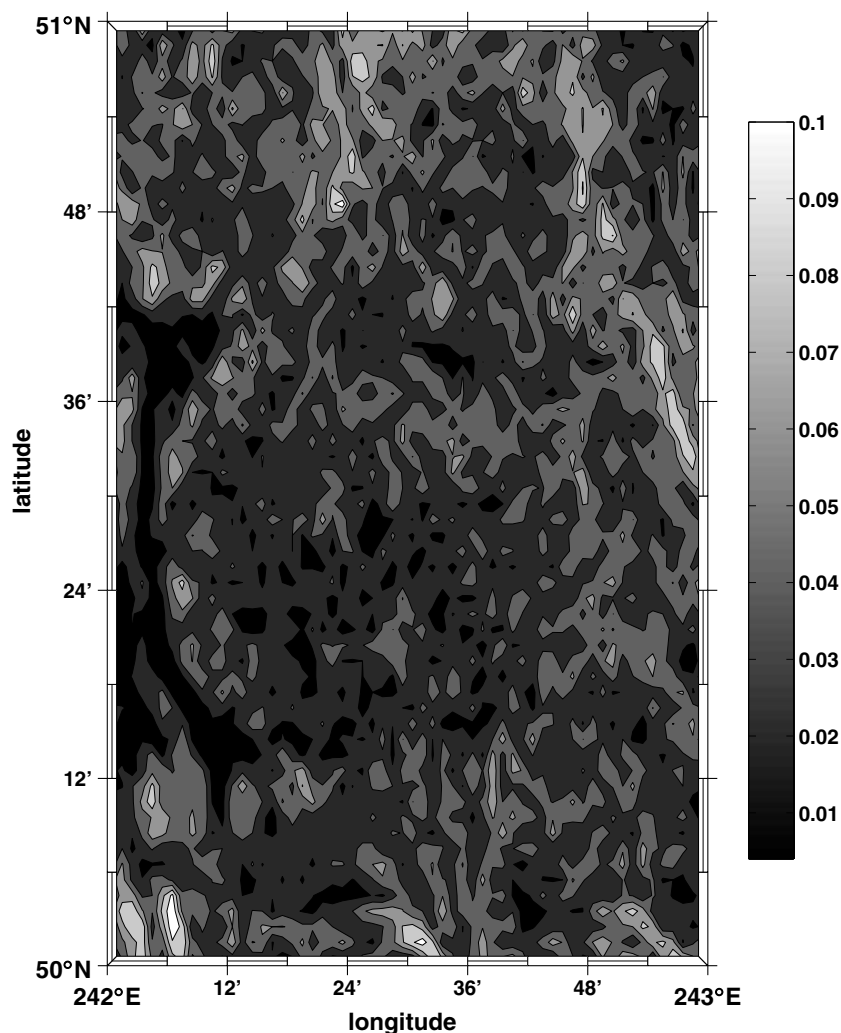$$\left. + \mathcal{N}^2(L, B, H, L^*, B^*) \right]^{1/2}.\text{(51)}$$

Fig. 6 Ellipsoidal correction to the spherical terrain gradient $\delta\Gamma^e$ (mGal)

The function $\mathcal{M}$ has the following form

$$
\begin{aligned}
\mathcal{M}&(L, B, H, L^*, B^*) \\
&= \left[X(L^*, B^*) - X(L, B, H) \right] \cos B^* \cos L^* \\
&\quad + \left[Y(L^*, B^*) - Y(L, B, H) \right] \cos B^* \sin L^* \\
&\quad + \left[Z(L^*, B^*) - Z(L, B, H) \right] \sin B^* .
\end{aligned} \tag{52}
$$

The distance $\mathcal{N}$ relates the computation point (L, B, H) and integration point at the ellipsoid (L^*, B^*)

$$
\begin{aligned}
\mathcal{N}(L, B, H, L^*, B^*) &= \Big\{ \left[X(L, B, H) - X(L^*, B^*) \right]^2 \\
&\quad + \left[Y(L, B, H) - Y(L^*, B^*) \right]^2 \\
&\quad + \left[Z(L, B, H) - Z(L^*, B^*) \right]^2 \Big\}^{1/2} .
\end{aligned} \tag{53}
$$

The Cartesian coordinates used in Eqs. (52) and (53) can easily be substituted from Eqs. (2). The three integrals in Eq. (10) can then easily be derived for the required integration limits from the primitive functions (integration constants as well as parameters of the functions $\mathcal{M}$ and $\mathcal{N}$ are omitted)

$$
\begin{aligned}
\mathcal{K}_1(L, B, H, L^*, B^*, \xi) &= \int_\xi \frac{1}{\mathcal{L}(L, B, H, L^*, B^*, \xi)} \, d\xi \\
&= \ln \left| \mathcal{M} + \xi + \mathcal{L}(L, B, H, L^*, B^*, \xi) \right| ,
\end{aligned} \tag{54}
$$

$$
\begin{aligned}
\mathcal{K}_2(L, B, H, L^*, B^*, \xi) &= \int_\xi \frac{\xi}{\mathcal{L}(L, B, H, L^*, B^*, \xi)} \, d\xi \\
&= \mathcal{L}(L, B, H, L^*, B^*, \xi) - \mathcal{M} \, \mathcal{K}_1(L, B, H, L^*, B^*, \xi) ,
\end{aligned} \tag{55}
$$

$$
\begin{aligned}
\mathcal{K}_3(L, B, H, L^*, B^*, \xi) &= \int_\xi \frac{\xi^2}{\mathcal{L}(L, B, H, L^*, B^*, \xi)} \, d\xi \\
&= \frac{1}{2} \Big[(\xi - 3\,\mathcal{M}) \, \mathcal{L}(L, B, H, L^*, B^*, \xi) \\
&\quad + \left(3\,\mathcal{M}^2 - \mathcal{N}^2 \right) \mathcal{K}_1(L, B, H, L^*, B^*, \xi) \Big] .
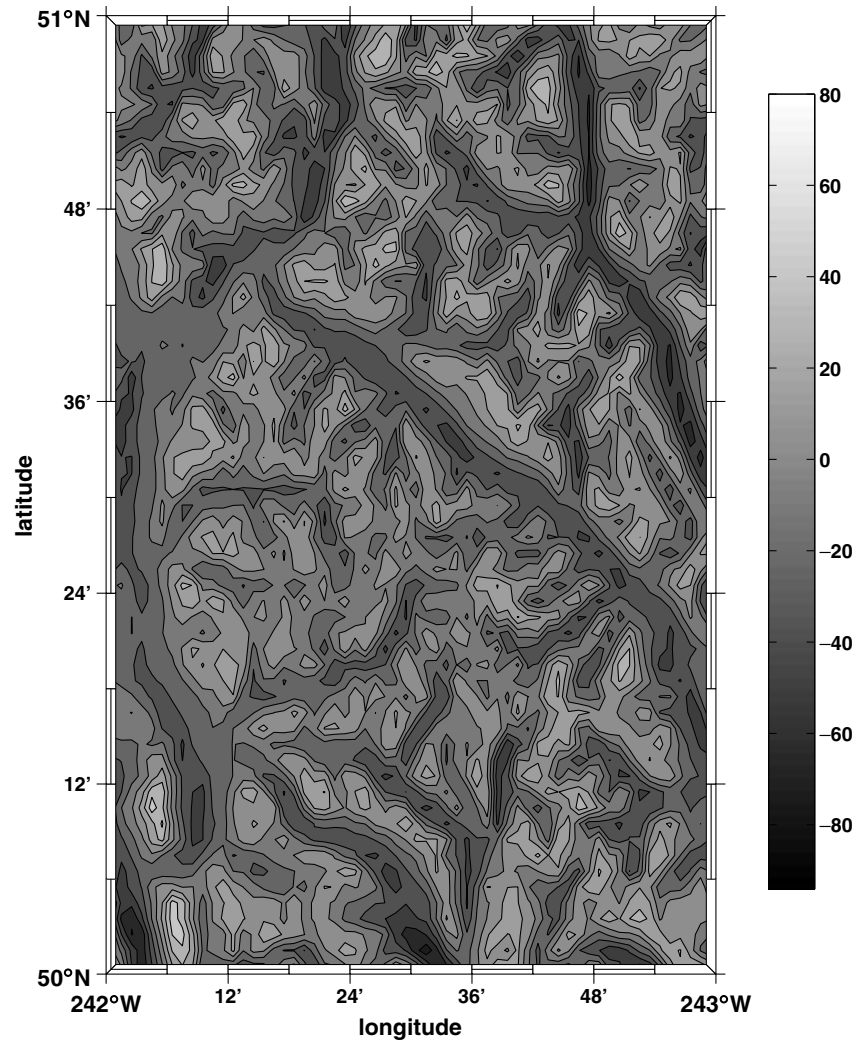\end{aligned} \tag{56}
$$

Fig. 7 Spherical condensed terrain gradient $\delta\Gamma^{cs}$ (mGal)

Appendix B

Singularity contributions of the ellipsoidal corrections

The singularity of the ellipsoidal correction to the spherical TP, see Eq. (15), is given for $H^* = H$

$$V_s^e(L, B, H) = G\varrho\, E^2 \int\limits_S \left[A^2\, \mathcal{K}_1(L, B, H, L^*, B^*, H) \right.$$
$$+ A\, \mathcal{K}_2(L, B, H, L^*, B^*, H) \Big]$$
$$\times \left(2\, \sin^2 B^* - 1\right)\, \mathrm{d}S + \mathcal{O}(E^4)\,. \qquad (57)$$

The integration kernels are, see Eq. (53) for definition of the function $\mathcal{N}$,

$$\mathcal{K}_1(L, B, H, L^*, B^*, H)$$
$$= \ln\left| \frac{\mathcal{M} + H + \mathcal{L}(L, B, H, L^*, B^*, H)}{\mathcal{M} + \mathcal{N}} \right|\,, \qquad (58)$$
$$\mathcal{K}_2(L, B, H, L^*, B^*, H) = \mathcal{L}(L, B, H, L^*, B^*, H)$$
$$- \mathcal{N} - \mathcal{M}\, \mathcal{K}_1(L, B, H, L^*, B^*, H)\,. \qquad (59)$$

Equation (57) represents deviations of the gravitational potential of a homogeneous Bouguer shell bounded by the reference ellipsoid and parallel surface separated at every point by the height H along the ellipsoidal normal from the potential of the homogeneous spherical shell. With respect to the size of the ellipsoid and thickness of the shell, this potential can well be approximated by the potential difference of two confocal homogeneous ellipsoids using the formulas of Pizzetti (1911) and Somigliana (1929). The counterpart to the potential V_s^e is the condensed ellipsoidal correction to the spherical CTP, see Eq. (30), defined for the same homogeneous shell

$$V_s^{ce}(L, B, H) = G\varrho\, A^2 E^2\, H\, \left(1 + \frac{H}{2A}\right)$$
$$\times \int\limits_S \frac{2\sin^2 B^* - 1}{\mathcal{N}(L, B, H, L^*, B^*)}\, \mathrm{d}S + \mathcal{O}(E^4)\,. \qquad (60)$$

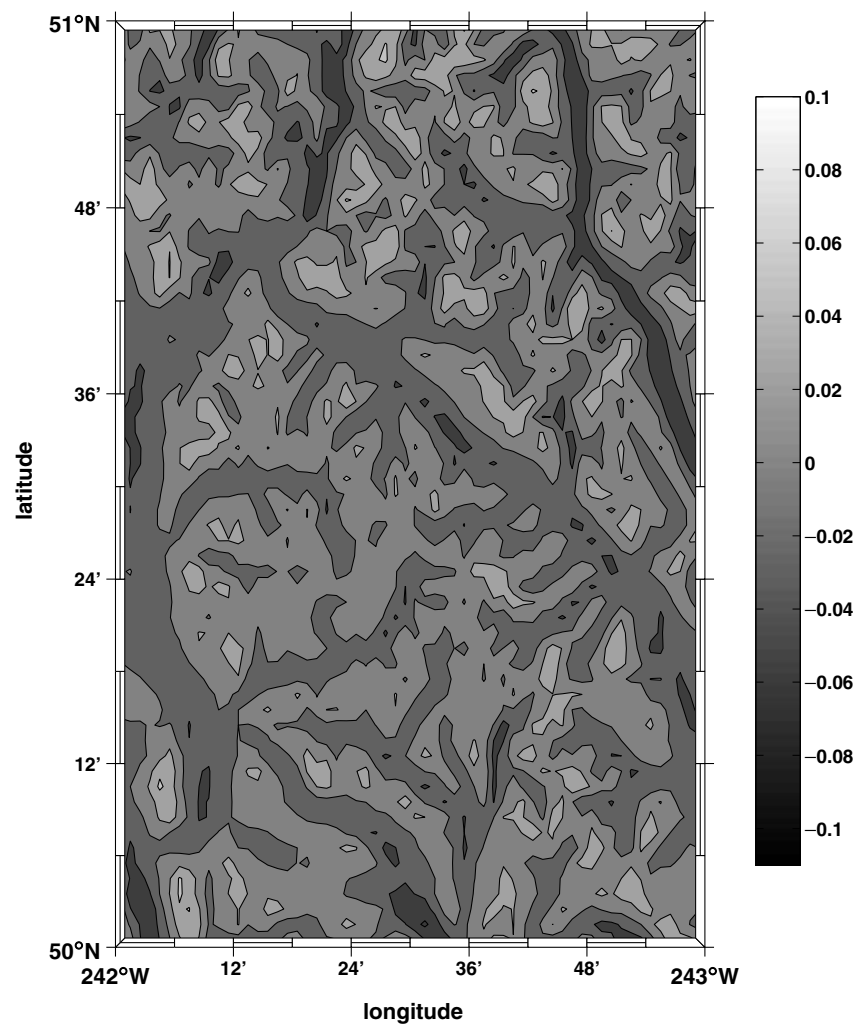For its evaluation, see Neumann (1887), Buchholz (1908), and Chandrasekhar (1969).

Fig. 8 Ellipsoidal correction to the spherical condensed terrain gradient $\delta\Gamma^{ce}$ (mGal)

Appendix C

Kernel functions $\mathcal{P}$

The directional derivative of the inverse distance function $\mathcal{L}$ can be derived in the form similar to the expression in Eq. (51)

$$\frac{\partial}{\partial H} \frac{1}{\mathcal{L}(L, B, H, L^*, B^*, \xi)}$$
$$= \frac{\mathcal{R}(L, B, H, L^*, B^*) + \mathcal{S}(L, B, L^*, B^*)\,\xi}{\mathcal{L}^3(L, B, H, L^*, B^*, \xi)} \,. \qquad (61)$$

The two new functions in Eq. (61) have the following form

$$\mathcal{R}(L, B, H, L^*, B^*)$$
$$= \left[X(L^*, B^*) - X(L, B, H) \right] \cos B \, \cos L$$
$$+ \left[Y(L^*, B^*) - Y(L, B, H) \right] \cos B \, \sin L$$
$$+ \left[Z(L^*, B^*) - Z(L, B, H) \right] \sin B \,, \qquad (62)$$

$$\mathcal{S}(L, B, L^*, B^*) = \cos B \, \cos L \, \cos B^* \, \cos L^*$$
$$+ \cos B \, \sin L \, \cos B^* \, \sin L^* + \sin B \, \sin B^* \,, \quad (63)$$

with the Cartesian coordinates defined in Eqs. (2). The functions $\mathcal{P}$ in Eq. (35) can be derived as follows (parameters of the functions $\mathcal{M}$, $\mathcal{N}$, $\mathcal{R}$ and $\mathcal{S}$ are omitted)

$$\mathcal{P}_1(L, B, H, L^*, B^*, \xi) = \int_\xi \frac{\partial}{\partial H} \frac{1}{\mathcal{L}(L, B, H, L^*, B^*, \xi)} \, d\xi$$

$$= \frac{\mathcal{R}\mathcal{M} - \mathcal{S}\mathcal{N}^2}{\left(\mathcal{N}^2 - \mathcal{M}^2 \right) \mathcal{L}(L, B, H, L^*, B^*, \xi)}$$

$$+ \xi \, \frac{\mathcal{R} - \mathcal{S}\mathcal{M}}{\left(\mathcal{N}^2 - \mathcal{M}^2 \right) \mathcal{L}(L, B, H, L^*, B^*, \xi)} \,, \qquad (64)$$

$$\mathcal{P}_2(L, B, H, L^*, B^*, \xi) = \int_\xi \frac{\partial}{\partial H} \frac{\xi}{\mathcal{L}(L, B, H, L^*, B^*, \xi)} \, d\xi$$

$$= \frac{\mathcal{R}\mathcal{N}^2 - \mathcal{S}\mathcal{N}^2\mathcal{M}}{\left(\mathcal{N}^2 - \mathcal{M}^2 \right) \mathcal{L}(L, B, H, L^*, B^*, \xi)}$$
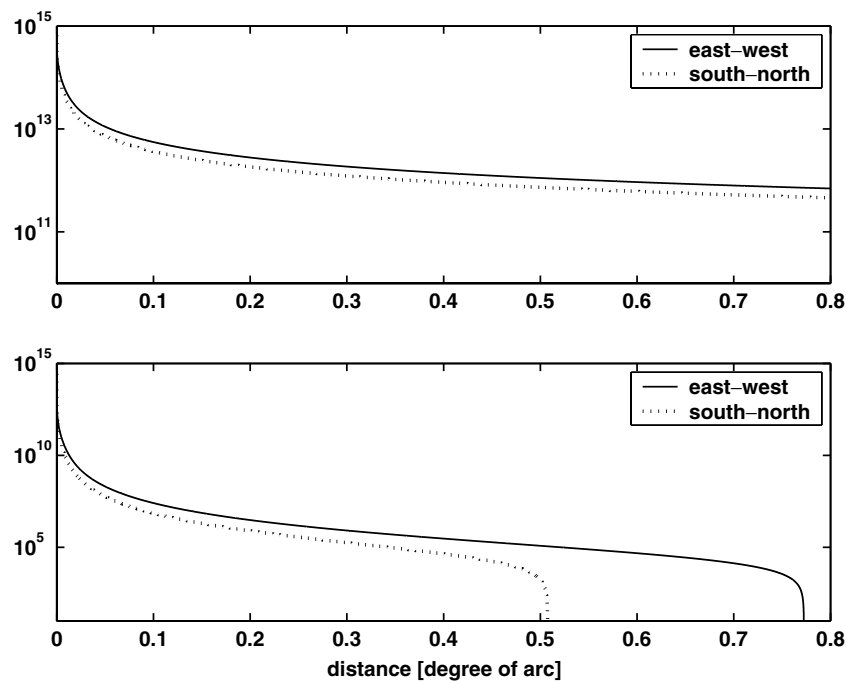
Fig. 9 Integration kernels for the potential (*TP*) and the potential gradient (*TPG*)

$$-\xi \, \frac{\mathcal{S}\mathcal{N}^2 + \mathcal{R}\mathcal{M} - 2\,\mathcal{S}\mathcal{M}^2}{\left(\mathcal{N}^2 - \mathcal{M}^2\right)\mathcal{L}(L, B, H, L^*, B^*, \xi)}$$
$$+\mathcal{S}\,\mathcal{K}_1(L, B, H, L^*, B^*, \xi), \tag{65}$$

$$\mathcal{P}_3(L, B, H, L^*, B^*, \xi) = \int\limits_\xi \frac{\partial}{\partial H} \frac{\xi^2}{\mathcal{L}(L, B, H, L^*, B^*, \xi)} \, d\xi$$

$$= \frac{2\,\mathcal{S}\mathcal{N}^4 + \mathcal{R}\mathcal{N}^2\mathcal{M} - 3\,\mathcal{S}\mathcal{N}^2\mathcal{M}^2}{\left(\mathcal{N}^2 - \mathcal{M}^2\right)\mathcal{L}(L, B, H, L^*, B^*, \xi)}$$

$$+\xi\,\frac{2\,\mathcal{R}\mathcal{M}^2 + 5\,\mathcal{S}\mathcal{N}^2\mathcal{M} - 6\,\mathcal{S}\mathcal{M}^3 - \mathcal{R}\mathcal{N}^2}{\left(\mathcal{N}^2 - \mathcal{M}^2\right)\mathcal{L}(L, B, H, L^*, B^*, \xi)}$$

$$+\xi^2\,\frac{\mathcal{S}}{\mathcal{L}(L, B, H, L^*, B^*, \xi)}$$

$$+(\mathcal{R} - 3\,\mathcal{S}\mathcal{M})\,\mathcal{K}_1(L, B, H, L^*, B^*, \xi). \tag{66}$$

Appendix D

Derivatives of the kernel functions $\mathcal{K}$

The first-order derivatives of the kernel functions $\mathcal{K}$ with respect to H^* in Eq. (47) are trivial. Assuming the same substitutions as in Appendix C, the second- and third-order derivatives of the integration kernels $\mathcal{K}$ can be derived as follows (parameters of the functions $\mathcal{M}$ and $\mathcal{N}$ are omitted):

$$\frac{\partial^2 \mathcal{K}_1(L, B, F, L^*, B^*, H^*)}{\partial H^{*2}}\bigg|_{H^*=H}$$
$$= -\frac{H + \mathcal{M}}{\mathcal{L}^3(L, B, F, L^*, B^*, H)}, \tag{67}$$

$$\frac{\partial^2 \mathcal{K}_2(L, B, F, L^*, B^*, H^*)}{\partial H^{*2}}\bigg|_{H^*=H}$$
$$= \frac{\mathcal{M}\,H + \mathcal{N}^2}{\mathcal{L}^3(L, B, F, L^*, B^*, H)}, \tag{68}$$

$$\frac{\partial^2 \mathcal{K}_3(L, B, F, L^*, B^*, H^*)}{\partial H^{*2}}\bigg|_{H^*=H}$$
$$= \frac{H^3 + 3\,\mathcal{M}\,H^2 + 2\,\mathcal{N}^2\,H}{\mathcal{L}^3(L, B, F, L^*, B^*, H)}, \tag{69}$$

$$\frac{\partial^3 \mathcal{K}_1(L, B, F, L^*, B^*, H^*)}{\partial H^{*3}}\bigg|_{H^*=H}$$
$$= \frac{2\,H^2 + 4\,\mathcal{M}\,H + 3\,\mathcal{M}^2 - \mathcal{N}^2}{\mathcal{L}^5(L, B, F, L^*, B^*, H)}, \tag{70}$$

$$\frac{\partial^3 \mathcal{K}_2(L, B, F, L^*, B^*, H^*)}{\partial H^{*3}}\bigg|_{H^*=H}$$
$$= -\frac{2\,\mathcal{M}\,H^2 + \mathcal{M}^2\,H + 3\,\mathcal{N}^2\,H + 2\,\mathcal{M}\,\mathcal{N}^2}{\mathcal{L}^5(L, B, F, L^*, B^*, H)}, \tag{71}$$

$$\frac{\partial^3 \mathcal{K}_3(L, B, F, L^*, B^*, H^*)}{\partial H^{*3}}\bigg|_{H^*=H}$$
$$= \frac{3\,\mathcal{M}^2\,H^2 - \mathcal{N}^2\,H^2 + 4\,\mathcal{M}\,\mathcal{N}^2\,H + 2\,\mathcal{N}^4}{\mathcal{L}^5(L, B, F, L^*, B^*, H)}. \tag{72}$$

Appendix E

Functions $\mathcal{J}$

The zero-order functions $\mathcal{J}$ in Eq. (49) can be computed by integration

$$\mathcal{J}_1^{(0)}(L, B, F, H) = \int_S \mathcal{K}_1(L, B, F, L^*, B^*, H)$$
$$\times \left[1 + E^2 \left(2 \sin^2 B^* - 1 \right) \right] \mathrm{d}S, \tag{73}$$

$$\mathcal{J}_2^{(0)}(L, B, F, H) = \int_S \mathcal{K}_2(L, B, F, L^*, B^*, H)$$
$$\times \left[2 + E^2 \left(2 \sin^2 B^* - 1 \right) \right] \mathrm{d}S, \tag{74}$$

$$\mathcal{J}_3^{(0)}(L, B, F, H) = \int_S \mathcal{K}_3(L, B, F, L^*, B^*, H) \, \mathrm{d}S. \tag{75}$$

The higher-order functions $\mathcal{J}$ for $i = 1, 2, 3 \ldots$ can be computed as

$$\mathcal{J}_{1,n,m}^{(i)}(L, B, F, H)$$
$$= \int_S \left[Z_{n,m}(L^*, B^*, E) - Z_{n,m}(L, B, E) \right]$$
$$\times \left. \frac{\partial \mathcal{K}_1(L, B, F, L^*, B^*, H^*)}{\partial H^{*i}} \right|_{H^*=H}$$
$$\times \left[1 + E^2 \left(2 \sin^2 B^* - 1 \right) \right] \mathrm{d}S, \tag{76}$$

$$\mathcal{J}_{2,n,m}^{(i)}(L, B, F, H)$$
$$= \int_S \left[Z_{n,m}(L^*, B^*, E) - Z_{n,m}(L, B, E) \right]$$
$$\times \left. \frac{\partial \mathcal{K}_2(L, B, F, L^*, B^*, H^*)}{\partial H^{*i}} \right|_{H^*=H}$$
$$\times \left[2 + E^2 \left(2 \sin^2 B^* - 1 \right) \right] \mathrm{d}S, \tag{77}$$

$$\mathcal{J}_{3,n,m}^{(i)}(L, B, F, H)$$
$$= \int_S \left[Z_{n,m}(L^*, B^*, E) - Z_{n,m}(L, B, E) \right]$$
$$\times \left. \frac{\partial \mathcal{K}_3(L, B, F, L^*, B^*, H^*)}{\partial H^{*i}} \right|_{H^*=H} \mathrm{d}S. \tag{78}$$

References

Buchholz H (1908) Das mechanische Potential und die Theorie der Figur der Erde. JA Barth, Leipzig

Chandrasekhar S (1969) Ellipsoidal figures of equilibrium. Yale University Press, New Haven London

Grafarend EW, Engels J (1992) A global representation of ellipsoidal heights – geoidal undulations or topographic heights – in terms of orthonormal functions. Manuscr Geod 17:52–58

Grafarend EW, Engels J (1993) The gravitational field of topographic-isostatic masses and the hypothesis of mass condensation. Surve Geophys 140:495–524

Grafarend EW, Ardalan A, Sideris MG (1999) The spheroidal fixed-free two-boundary-value problem for geoid determination (the spheroidal Bruns' transform). J Geod 73:513–533

Heck B (2003) On Helmert's methods of condensation. J Geod 77:155–170

Huang J, Vaníček P, Brink W, Pagiatakis S (2001) Effect of topographical mass density variation on gravity and the geoid in the Canadian Rocky Mountains. J Geod 74:805–815

Lelgeman D (1970) Untersuchungen zu einer genaueren Lösung des Problems von Stokes. Deutsche Geodätische Kommission, Reihe C, Nr. 155

MacMillan WD (1958) The theory of the potential. Dover, New York

Martinec Z (1998) Boundary-value problems for gravimetric determination of a precise geoid. Lecture notes in Earth Sciences, Vol 73. Springer, Berlin Heidelberg New York

Martinec Z, Vaníček P (1994) Direct topographical effect of Helmert's condensation for a spherical approximation of the geoid. Manuscr Geod 19:257–268

Moritz H (1984) Geodetic reference system 1980. Bull Géod 58:388–398

Neumann F (1887) Vorlesungen über die Theorie des Potentials und der Kugelfunctionen. BG Teubner, Leipzig

Novák P (2000) Evaluation of gravity data for the Stokes-Helmert solution to the geodetic boundary-value problem. Tech Rep 207, Department of Geodesy and Geomatics Engineering, University of New Brunswick, Fredericton

Novák P, Vaníček P, Martinec Z, Véronneau M (2001) Effects of the spherical terrain on gravity and the geoid. J Geod 75:491–504

Novák P, Vaníček P, Véronneau M, Holmes SA, Featherstone WE (2001) On the accuracy of Stokes's integration in the precise high-frequency geoid determination. J Geod 74:644–654

Novák P, Kern M, Schwarz KP, Heck B (2003) Evaluation of band-limited topographical effects in airborne gravimetry. J Geod 76:597–604

Pizzetti P (1911) Sopra il Calcolo Teorico delle Deviazioni del Geoide dall'Ellisoide. Atti Reale Accademia delle Scienze 46, Torino

Somigliana C (1929) Teoria Generale del Campo Gravitazionale dell'Ellisoide di Rotazione. Memoire della Societa Astronomica Italiana 4, Milano

Vaníček P, Novák P, Martinec Z (2001) Geoid, topography, and the Bouguer plate or shell. J Geod 75:210–215